RTDS Evaluation of Time-Domain Line Protection Performance Applied on a Transmission Line With High Complexity

Denise Borges de Oliveira, Tatiana Maria Tavares de Souza Alves, and Alex Castro
Operador Nacional do Sistema Elétrico

Antônio Carlos Duarte
Independent Consultant

Felipe Lopes and Tiago Honorato
Universidade de Brasília

Andrei Coelho and Paulo Lima
Schweitzer Engineering Laboratories, Inc.

Revised edition released November 2022

Originally presented in Portuguese at the
XV Seminário Técnico de Proteção e Controle
(Protection and Control Technical Seminar), October 2021

RTDS Evaluation of Time-Domain Line Protection Performance Applied on a Transmission Line With High Complexity

Denise Borges de Oliveira, Tatiana Maria Tavares de Souza Alves,
and Alex Castro, *Operador Nacional do Sistema Elétrico*
Antônio Carlos Duarte, *Independent Consultant*
Felipe Lopes and Tiago Honorato, *Universidade de Brasília*
Andrei Coelho and Paulo Lima, *Schweitzer Engineering Laboratories, Inc.*

***Abstract*—The purpose of this paper is to present the outcomes of using time-domain line-protection technology on the highly complex 500 kV transmission line that connects the Xingu and Tucuruí substations in Brazil. The transmission line is a long, double-circuit line with both series and shunt reactive compensation in the proximity of high-voltage direct current (HVDC) links. The system was modeled in a real-time digital simulator (RTDS) and in Alternative Transients Program (ATP) software to simulate system events as realistically as possible. The paper also features results from real events collected from the field and reapplied to relays that use time-domain technology of traveling waves and incremental quantities.**

I. Introduction and System Overview

The 500 kV Xingu-Tucuruí transmission line consists of two 265 km (165 mi) parallel circuits with series capacitors at the Xingu terminal. These capacitors have a 70 percent compensation level. In Xingu, there are two high-voltage direct current (HVDC) bipoles associated with the Belo Monte Hydroelectric Plant (±800 kV) that lead to the Estreito and Terminal Rio inverter stations. In addition, this line crosses the Amazon region, where vegetation includes many tall and fast-growing trees that can cause high-resistance faults. There is also strong mutual coupling between adjacent 500 kV lines that share the same tower, which are also compensated.

Considering all of these points, the conventional phasor-based protection systems of this line are susceptible to undesired performance problems. These problems can result from the presence of subharmonic frequencies, the inversion of voltage and current caused by the presence of series capacitor banks, and/or the mutual coupling and grounding factors of the electrical network.

The appearance of unbalanced currents and voltages with a high-harmonic content also influences the performance of the line-protection system after the elimination of external short circuits, which can be attributed to the phenomenon of converter transformer recovery inrush at the Xingu station. Proximity to the HVDC link can also cause the line protection to misoperate when switching faults occur in the inverter station following short circuits in the Southeast region of the country close to the Estreito or Terminal Rio substations [1]. These switching faults cause large fluctuations in current and voltage and, consequently, cause large deviations in the apparent impedance measured by the protection relay for the line under study. This results in transient overreaches of phasor-based distance protection elements.

Thus, considering the complexity of the line and the effect of harsh conditions on the performance of conventional phasor protection, Operador Nacional do Sistema Elétrico (ONS) decided to test time-domain line protection on the 500 kV Xingu-Tucuruí C1 transmission line using a real-time digital simulator (RTDS) and Alternative Transients Program (ATP) software to evaluate its performance.

II. RTDS Model

An RTDS was used to simulate the system. Due to the network arrangement, the smallest possible integration step was 6 μs for the small time-step block. The line used in the test had transposition at 1/6, 1/3, 1/3, and 1/6. It was modeled using the frequency-dependent line model (J. Marti model).

Generation was modeled on the Belo Monte, Tucuruí 1, and Tucuruí 2 nodes; the following busbars were also modeled later:

- Oriximiná (500 kV)
- Jurupari (500 kV)
- Jurupari (230 kV)
- Belo Monte (500 kV)
- Xingu (500 kV)
- Xingu (230 kV)
- Tucuruí (230 kV)
- Tucuruí (500 kV)
- Vila do Conde (500 kV)
- Itacaiúnas (500 kV)
- Marabá (500 kV)
- Colinas (500 kV)
- Imperatriz (500 kV)
- Miracema (500 kV)

The rest of the system was represented by an equivalent network. The diagram of the area modeled in the RTDS simulation is shown in Fig. 1. The analyzed line, Circuit 1 connecting Xingu and Tucuruí, is highlighted in blue.

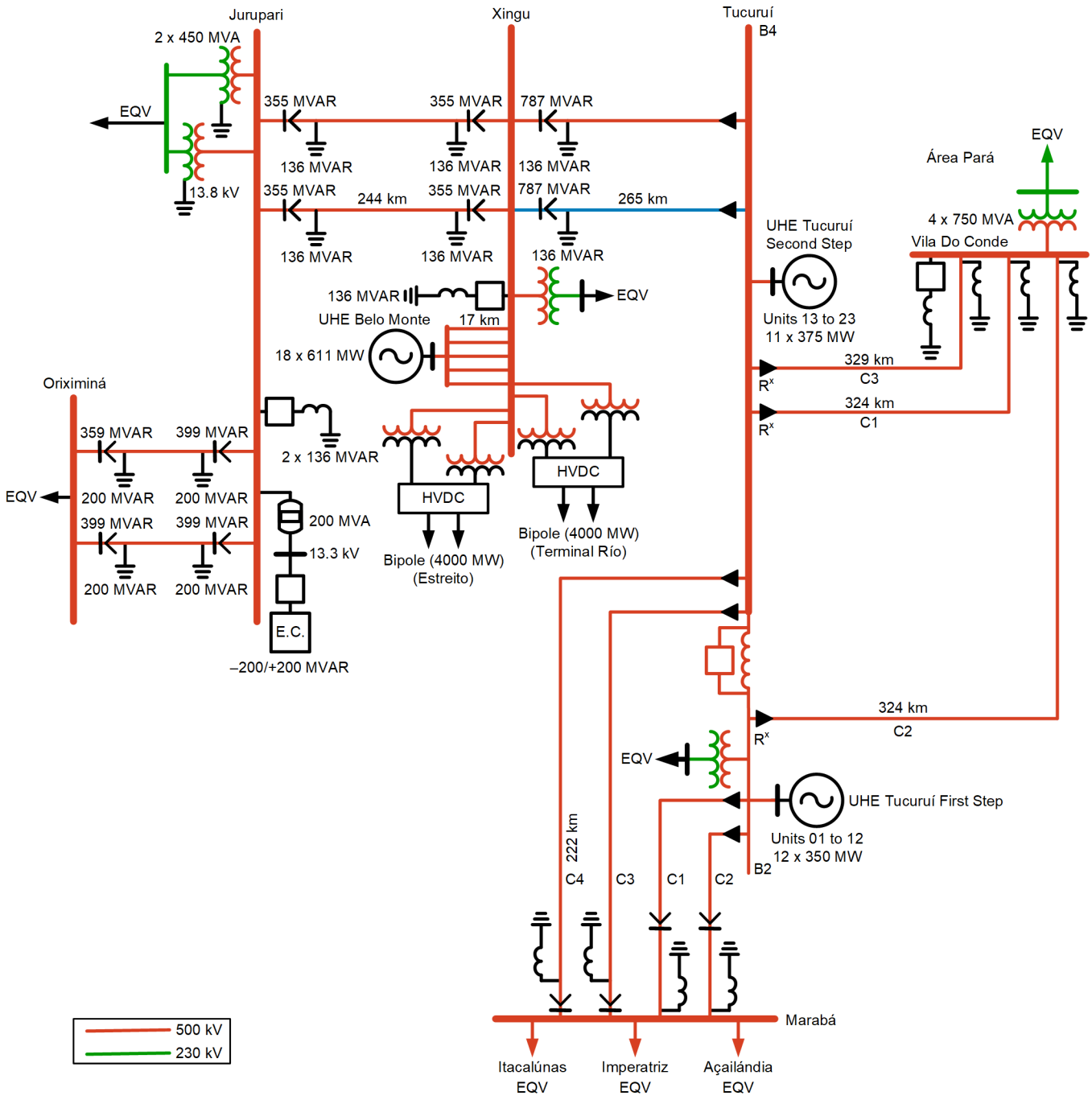

Fig. 1. One-line diagram of the RTDS-modeled system. The line being studied is in blue.

III. Analysis of RTDS Case Study Results

This section presents the results obtained during RTDS testing. Table I summarizes all test cases.

TABLE I
RTDS TEST CASES

Case Number	Description		
	Disturbance Type	Fault Type	Location
01	Internal fault	AG	16.67% from Xingu terminal
02	Internal fault	AG	50% from Xingu terminal
03	Internal fault	AG	83.33% from Xingu terminal
04	External fault	AG	Parallel circuit. 16.67% from Xingu terminal
05	External fault	AG	Parallel circuit. 50% from Xingu terminal
06	External fault	AG	Parallel circuit. 83.33% from Xingu terminal
07	External fault	AG	Xingu busbar
08	External fault	AG	Tucuruí busbar
09	External fault	AG	Belo Monte busbar
10	External fault	AG	Marabá busbar
11	External fault	AG	Jurupari busbar
12	External fault that evolves into internal fault		50% from Xingu terminal
13	Internal fault	ABC	16.67% from Xingu terminal
14	Internal fault	ABC	50% from Xingu terminal
15	Internal fault	ABC	83.33% from Xingu terminal
16	External fault	ABC	Parallel circuit. 16.67% from Xingu terminal
17	External fault	ABC	Parallel circuit. 50% from Xingu terminal
18	External fault	ABC	Parallel circuit. 83.33% from Xingu terminal
19	External fault	ABC	Xingu busbar
20	External fault	ABC	Tucuruí busbar
21	External fault	ABC	Belo Monte busbar
22	External fault	ABC	Marabá busbar
23	External fault	ABC	Jurupari busbar
24	Internal fault	AG	83.33% from Xingu terminal with fault resistance
25	Switching		Series capacitor bank bypass
26	Switching		Energization of converter transformers
27	Playback		Playback—fault on Belo Monde Busbar
28	Playback		Playback—HVDC switching failure

A. Internal Faults

This line has transposition, and these points were used to apply internal faults. The fault points were 16.67 percent, 50 percent, and 83.33 percent of the line length from the Xingu substation. Internal single-line-to-ground and three-phase faults were applied at these points with incidence angles of 0 degrees and 90 degrees. The functions TD21, TW87, and permissive overreaching transfer trip (POTT) (using TD32 and TW32 as directional elements) were enabled to trip, and for all simulations, the ultra-high-speed protection performed as expected. Table II summarizes the average operating times obtained for each function, as well as the average trip time, disregarding channel latencies. All protection functions are detailed in [2] and [3].

TABLE II
AVERAGE OPERATING TIMES FOR INTERNAL FAULTS

Protection Function	Average Operating Time (ms)
TD32	1.8
TD21	2.6
TW32	0.1
TW87	1.2
TRIP	1.7

Fig. 2 shows the results of one of the tests, Case 3, which was a bolted single-line-to-ground fault at 83.33 percent of the line from the Xingu substation.

Fig. 2a

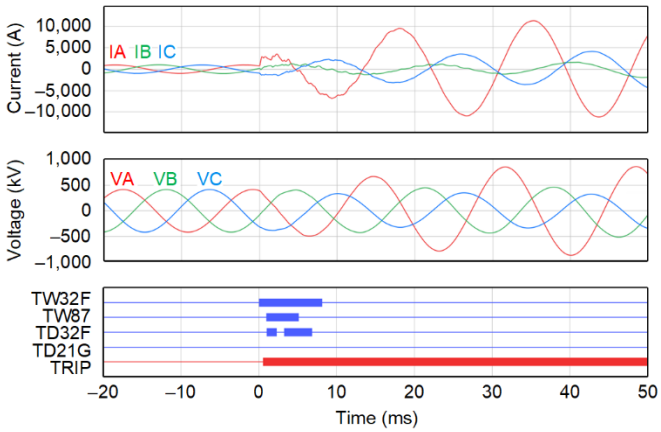

Fig. 2b

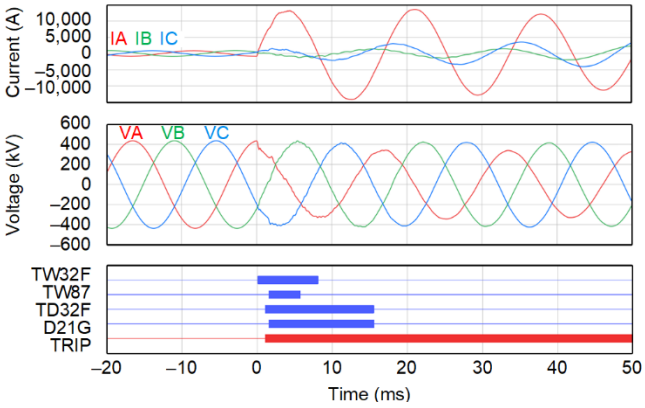

Fig. 2. Event record oscillography and digital data showing results for internal fault at (a) Xingu and (b) Tucuruí relays.

At both line terminals, engineers observed that both the traveling-wave directional element and the incremental-quantity directional element declare a forward direction (assertion of TW32F and TD32F, respectively). The ground incremental-quantity distance element (TD21G) operated for the substation closest to the fault, as expected. The traveling-wave differential scheme (TW87) also detected this fault at both terminals. All protection elements operated rapidly for an ultra-high-speed trip of the relay.

Fig. 3 shows Case 24, a fault with resistance equal to 150 ohms at 83.33 percent from the Xingu substation. In this scenario, the TD32F element was asserted in both relays; hence, the correct performance of the POTT scheme was observed and caused both relays to issue a trip signal.

Fig. 3a

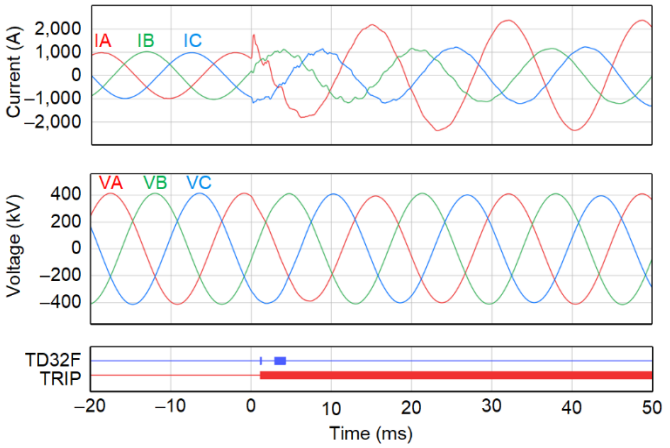

Fig. 3b

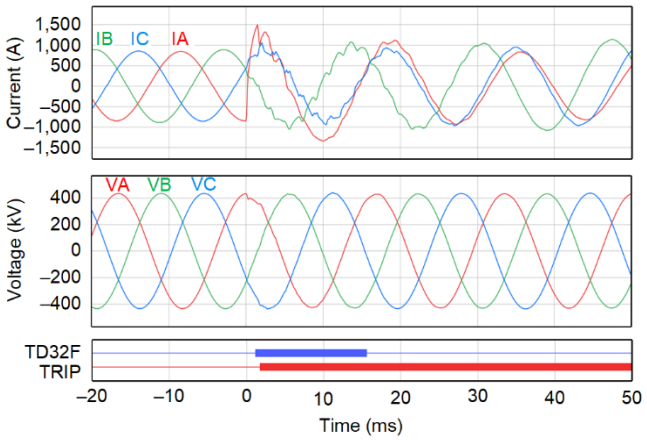

Fig. 3. Case 24 oscillography and digital data showing TD32F and TRIP assertions for (a) Xingu and (b) Tucuruí relays.

High-impedance fault-detection sensitivity is dependent on the selected settings. Choosing more sensitive settings allows the detection of higher impedance faults but compromises security. Normally, impedances of 100 ohms are used to calculate settings for single-line-to-ground faults, considering the worst condition of the power system, in terms of fault-current contribution (i.e., source behind the relay is at its expected weakest value and remote source is at its expected strongest value). The settings definition in this paper uses this methodology.

B. *External Faults*

Table I shows a great number of external faults applied to verify protection security and to protect against undesired tripping in this system, which can occur frequently with phasor-based protection. For all external faults tested on time-domain relays, operation remained secure. Fig. 4 shows an example of a fault on the midpoint of the parallel circuit, Case 5, for which the relays performed as expected.

Fig. 4a

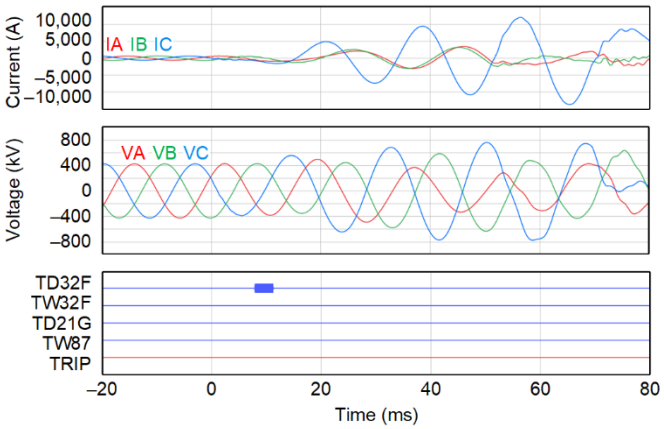

Fig. 4b

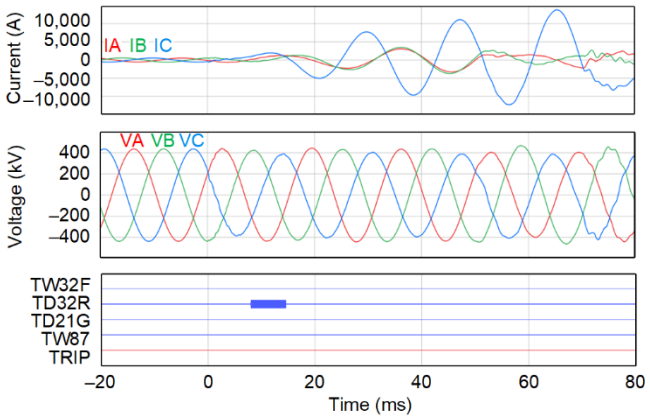

Fig. 4. Case 5 oscillography and digital data obtained at (a) Xingu and (b) Tucuruí relays.

All elements were secure for this case. The TD32 directional element detected a fault forward at the strong source terminal, Xingu substation. At the weak source terminal, Tucuruí substation, TD32 detected the fault as reverse, meaning the POTT scheme was secure.

C. *Fault Evolving From External to Internal*

Time-domain protection elements, using the principles of incremental quantities and traveling waves, need to measure stable electrical quantities to become armed prior to a disturbance. Once a disturbance occurs, the time-domain protection elements become disarmed until a new steady-state condition is reached and the relay becomes armed again. During an external fault, the relay executes its algorithms, does not operate, and remains secure. If the fault develops into an internal fault, then the relay must calculate new incremental quantities. Thus, in the case of a second fault (the internal fault),

the pre-fault is a system fault (the external fault). In this case, it is necessary to set a time delay in the software simulation that allows the external fault to reach the permanent short-circuit state for a period of time before transitioning to the internal fault. The time during which the relay disables the arming of protection (i.e., the arming logic) is determined by both a fixed minimum time and a variable time that is determined according to system-stabilization time constants. Fig. 5 shows the results of Case 12, which is an external fault that initiated in the middle of the parallel circuit and evolved into an internal fault.

Fig. 5a

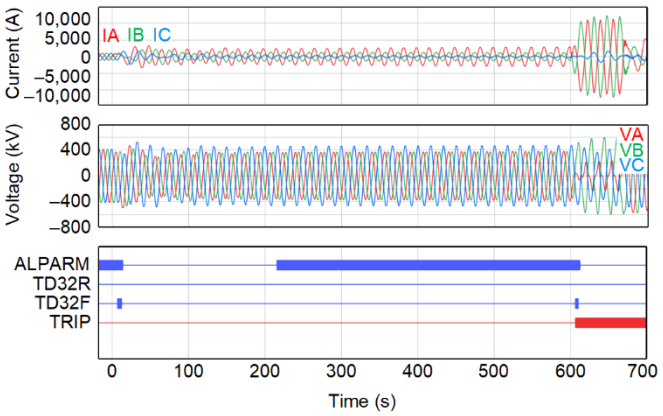

Fig. 5b

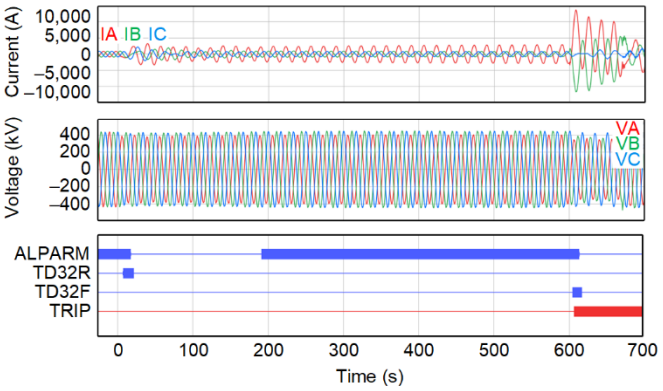

Fig. 5. Case 12 oscillography and digital data from the (a) Xingu substation and (b) Tucuruí substation relays. A fault on the parallel circuit evolves into an internal fault; the system remains secure.

Fig. 5 shows the behavior of the TD32 element in each relay. The Xingu substation relay detected both internal and external faults as forward faults. The Tucuruí substation relay correctly detected the first fault as reverse and the second fault as forward. The ALPARM variable, shown in Fig. 5, represents the moments when the relay protection was armed and the incremental-quantity-based elements (and TW-based elements) were active.

The fault in Fig. 5 was sustained for almost 600 milliseconds, which is typical. Similar tests were performed with elimination of the parallel line fault with identical results. The relays were available to provide protection after the electrical input signals returned to a quiescent state. For the tested fault conditions, the duration of inactive protection was 175 milliseconds (ALPARM deasserted).

D. Capacitor Bank Bypass

In addition to faults, the insertion and removal of the capacitor bank, which is within the protection zone, was also simulated. These switching events did not activate the protection trip because they were not faults, but they did generate incremental quantities and traveling waves on the line. Again, the relay restrained and remained secure. Fig. 6 shows the result for the capacitor bank bypass, Case 25.

Fig. 6a

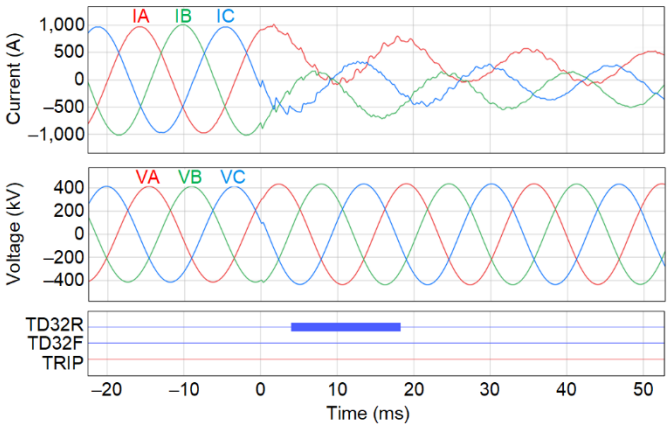

Fig. 6b

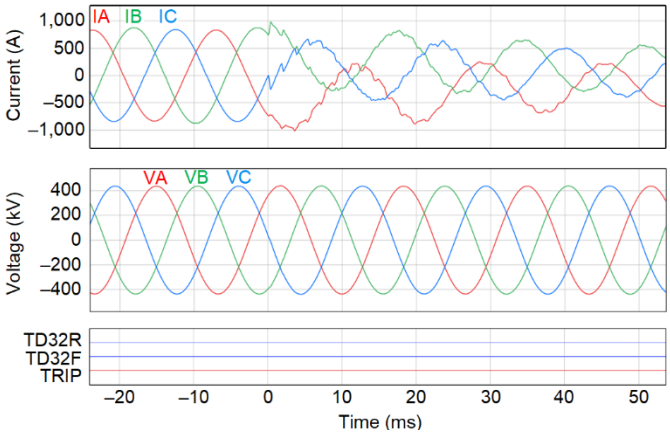

Fig. 6. Case 25 oscillography and digital data from the (a) Xingu substation and (b) Tucuruí substation relays. By bypassing the capacitor bank, the system remains secure.

The Xingu substation calculated this event as reverse, since the bank is behind the relay potential transformer. The Tucuruí substation detected this event in the forward direction; however, its calculations were such that the transients generated by the bypassing of the capacitor bank were not sufficient to activate the directional algorithm. In summary, the performance of the protection scheme was correct and secure.

E. HVDC Switching Failure

This case involves a switching failure of an HVDC link that occurred in the power system and was captured by devices installed in the field. The real field records were reapplied using the event playback feature that is built into these time-domain relays. There was a fault in the ac system near an inverter substation (in the southeastern region) that is located more than 2,000 km (1,242 mi) away from the evaluated transmission line,

which resulted in the dipole failing to switch. The switching failure cut off active power transferred through the link, and this momentary event caused the misoperation of the phasor-based protection installed on the line. Fig. 7 shows the response of the time-domain relays at both line terminals.

Fig. 7a

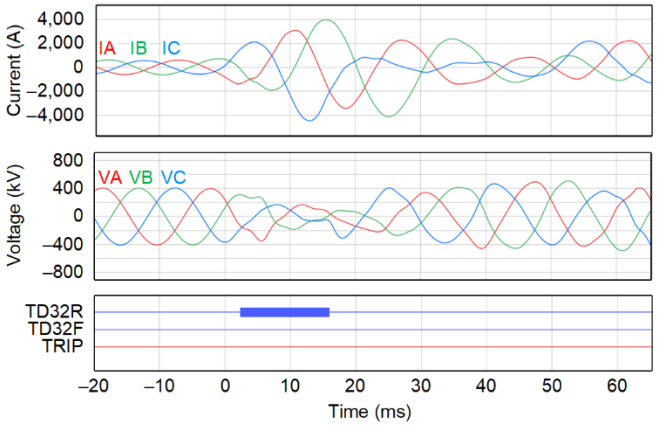

Fig. 7b

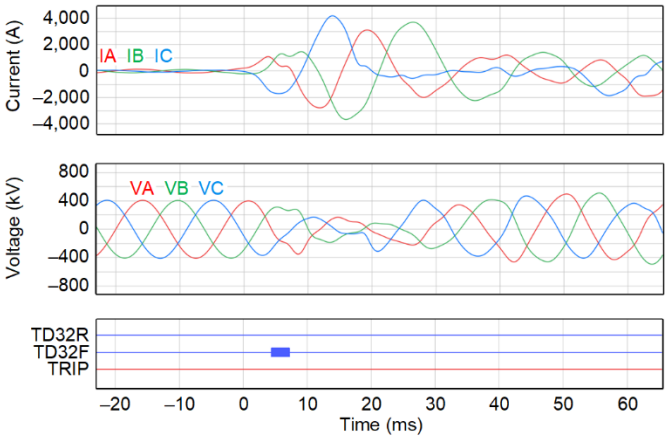

Fig. 7 Results obtained from the switching failure of the HVDC link at the (a) Xingu substation and (b) Tucuruí substation relays.

The time-domain relays did not signal a trip and, since the event was detected in the forward direction (TD32F) by one terminal and in the reverse direction (TD32R) by the other, the relays were secure. Also, the oscillographs in Fig. 7 show current interruption, the result of phasor-based relays insecurely tripping the circuit breakers.

IV. Extensive ATP Testing

To comprehensively analyze the performance of the time-domain protection elements, extensive tests were performed using computer simulations of faults in the same test system evaluated in the previous sections. For these tests, ATP was used for detailed modeling of the monitored electrical network. Through the simulations in ATP, oscillographs were generated with a sampling rate of 1 MHz, compatible with the event-playback testing functionality of the time-domain relays [4]. Automation of the tests was carried out using the methodology reported in [5].

Three groups of tests were evaluated:

- Test Group 1: 256 simulated internal faults on the protected line
- Test Group 2: 128 simulated external faults on the parallel line
- Test Group 3: 76 simulated external faults on the 500 kV Tucuruí–Jurupari line

All cases were evaluated using the frequency-dependent line model (J. Marti model). In Test Groups 1 and 2, the positions of the applied faults were varied in terms of the percentage of the length of each transposed section. In Test Group 3, the position of the fault was varied in terms of percentage of the total length.

Table III shows the fault parameters in each group of simulation tests, which were chosen to evaluate reliability of the protection scheme. Protection reliability is a measure of the degree of certainty that the relay, or relay system, will perform (operate) correctly (dependably) for internal faults together with assurance against incorrect operation (security) from all extraneous causes, such as switching events and external faults. Hence, we measure:

- Dependability—the ability of the scheme to respond to all internal faults.
- Security—the ability of a protection scheme to avoid operation for external fault conditions.

The results obtained are presented in terms of the percentage of protection element operations in relation to the number of simulated cases (see Fig. 8), as well as the probability distribution of the operating times in relation to the fault location (see Fig. 9). In all analyses, results obtained at both terminals of the protected line are presented. It is also noteworthy that, during laboratory tests, the communication between relays was implemented via optical fiber approximately two meters long, so that the latency of the channel could be considered negligible.

TABLE III
SIMULATED FAULT PARAMETERS

Test Groups	Fault Type	Distance to Fault (% of Line From Reference Terminal)*	Phase-Ground Fault Resistance	Phase-to-Phase Fault Resistance	Incidence Angle**
1	Internal AG, AB, ABG, and ABC	20% to 80%, Δ = 20% (per transposition section)	≈ 0 ohms and 50 ohms	≈ 0 ohms and 20 ohms	0° and 90°
2	External AG, AB, ABG, and ABC	20% to 80%, Δ = 20% (per transposition section)	≈ 0 ohms	≈ 0 ohms	90°
3	External AG, AB, ABG, and ABC	5% to 95%, Δ = 5% (along the whole transmission line)	≈ 0 ohms	≈ 0 ohms	90°

* Δ = step of variation of the fault location; ** Sinusoidal angle reference in Phase A

Fig. 8a

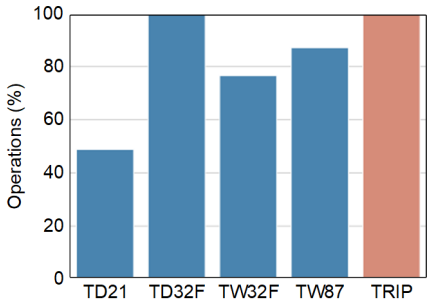

Fig. 8b

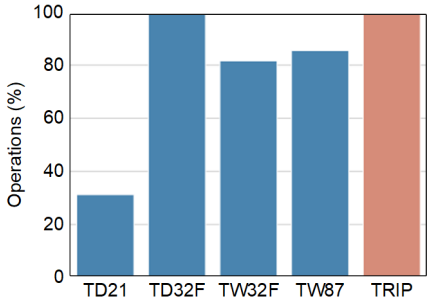

Fig. 8 Percentage of operations for internal faults (Test Group 1) at (a) Tucuruí and (b) Xingu.

A. Results Obtained for Internal Faults (Test Group 1)

From Fig. 8, the trip output activated in 100 percent of the cases. Likewise, TD32F operated in all scenarios evaluated at both terminals of the line, producing POTT scheme operations. The TW32F and TW87 elements operated in more than 80 percent of the cases in Tucuruí and Xingu, with highly damped transients being the only conditions they were not sensitized to. Regarding the TD21 function, there were operations in approximately 49 percent and 32 percent of cases in Tucuruí and Xingu, respectively. Such percentages were expected due to the TD21 being an underreaching element whose sensitivity reduces for faults with high resistance. Even so, in the cases in which it operated, TD21 resulted in maximum reaches of 70 percent and 43 percent in relation to the Tucuruí and Xingu terminals, respectively.

In Fig. 9, the probability distributions of the operating times of elements TD21, TD32F, TW32F and TW87 are presented in relation to the fault location. The underreaching nature of the TD21 element is confirmed, which showed a higher probability of operations in less than 6 milliseconds in Tucuruí and 4.5 milliseconds in Xingu. Regarding elements TD32, TW32 and TW87, it appears that each could identify short circuits over the entire length of the transmission line. In terms of operating times, when considering the highest probabilities obtained for the evaluated system, times shorter than 2.7 milliseconds and 3.5 milliseconds were found for the TD32F in Tucuruí and Xingu, respectively, as well as 1.0 milliseconds and 3.0 milliseconds for TW32F and TW87, respectively, at both line terminals. Given these results, it is confirmed that the evaluated elements were capable of providing reliable and ultra-high-speed performance, even when applied to more complicated electric power transmission system networks.

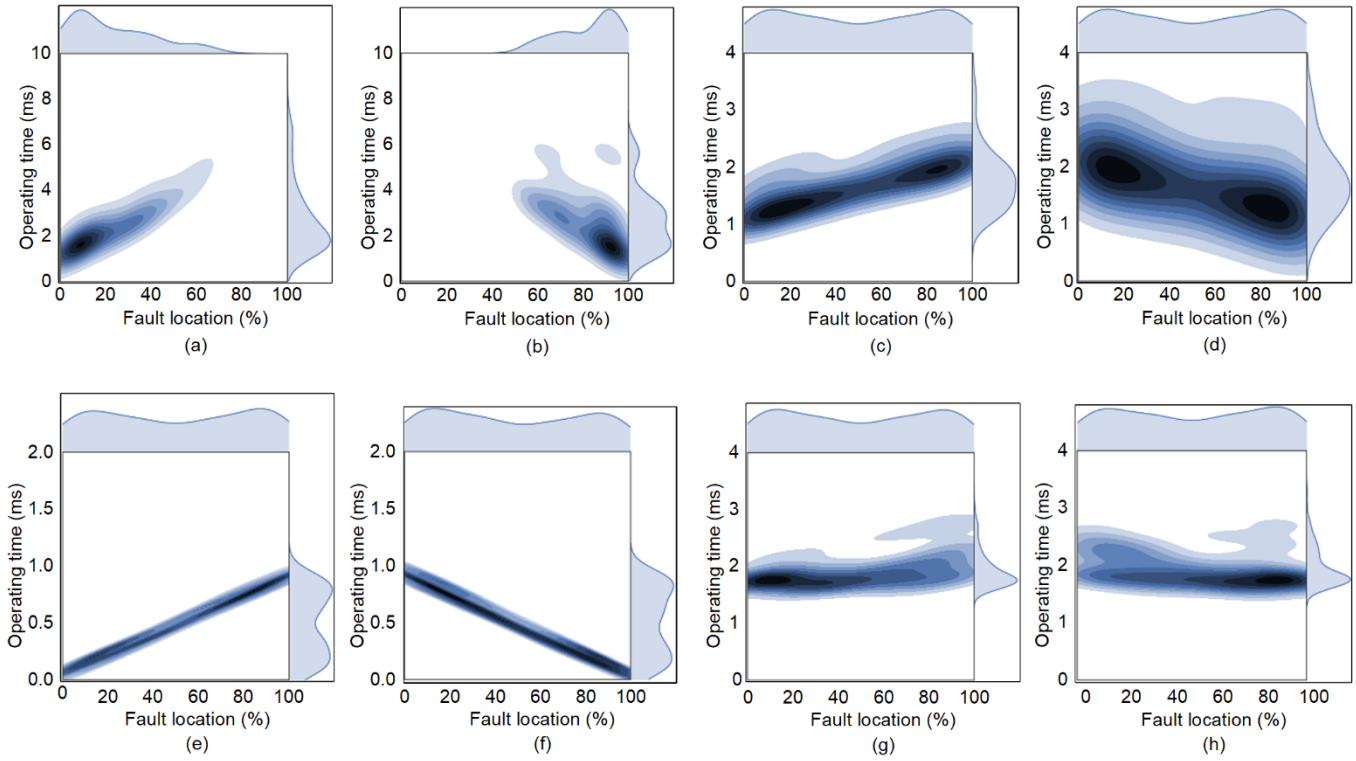

Fig. 9 Two-variable contour probability-density plot, showing operating times in relation to the fault location: (a) TD21 in Tucuruí; (b) TD21 in Xingu; (c) TD32F in Tucuruí; (d) TD32F in Xingu; (e) TW32F in Tucuruí; (f) TW32F in Xingu; (g) TW87 in Tucuruí; (h) TW87 in Xingu.

B. *Results Obtained for External Faults (Test Groups 2 and 3)*

The results obtained from the analysis of external faults in Test Groups 2 and 3 are presented together in Fig. 10. Since the actions of the evaluated protection schemes were not expected, the results are illustrated only in terms of the percentage of operations. As demonstrated, only the TD32F element operated in some scenarios, which, depending on the location of the simulated short circuit, was expected. Even so, undesired remote permissive signals were not observed, and in all cases the trip command was restrained through the POTT scheme. Thus, the TRIP variable remained at zero percent of operations (which consists of TD21, POTT, and TW87), demonstrating that undesired trip commands did not occur because, in all scenarios, the evaluated elements were secure.

Fig. 10a

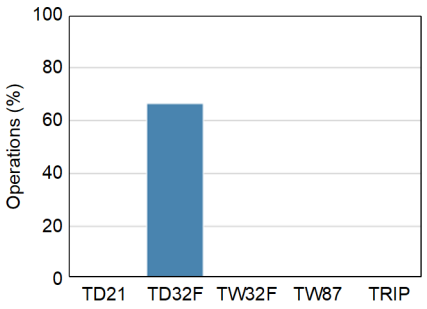

Fig. 10b

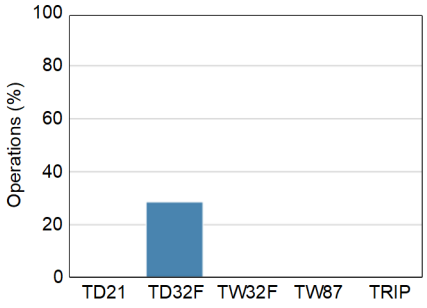

Fig. 10 Percentage of operations for cases in Test Groups 2 and 3 at (a) Tucuruí and (b) Xingu.

V. Conclusion

This paper presented an analysis of the simulated performance of time-domain protection in a highly complex region of the National Interconnected System (SIN) of Brazil. This region was chosen specifically because it experiences many system events that can compromise the performance of applied phasor protection. A challenging scenario like this can be considered ideal for testing any technology that seeks to increase the safety and reliability of an electric power system.

These tests utilized simulations created in RTDS and ATP. The focus of the ATP simulations was to produce results for a large volume of cases with which to test all types of faults in various fault locations and with fault-impedance variations. In contrast, the RTDS testing sought to examine carefully selected cases with a more detailed analysis of the results. It appears that most scenarios tested in RTDS refer to situations of external faults or system transients, which can generate security challenges for phasor-based protection.

For all cases tested in both RTDS and ATP, time-domain protection performed as expected. It operated with a high level of dependability and sensitivity for internal faults. This includes faults with high fault impedance, up to 150 ohms, a value higher than expected based on the selected settings. In addition, protection remained secure for all external faults or switching events, as expected.

The companion phasor-based protection was responsible for the actions taken during events in which protection in the time-domain was not armed and there was an internal fault, such as an evolving fault that was shorter than the duration required to assert the arming logic that supervises the time-domain protection.

For internal faults, the ultra-high-speed performance of the tested protection system was confirmed, which is beneficial. Average trip times were less than 2 milliseconds. Benefits of fast tripping include reduced equipment damage, increased system stability, and ultra-high-speed operation in highly complex systems, which further improve the safety and reliability of the electric power system. During short circuits, there are voltage and current inversions, asymmetric bank bypasses, CT saturation, etc. All these conditions hinder the algorithms of microprocessor- and phasor-based protection relays. Algorithms that detect and respond quickly, before these effects can even occur, improve performance.

Considering these results, time-domain protection has proven itself a great solution for providing better security and dependability in the evaluated system and is likely a promising technology for other systems with highly complex topologies and conditions.

VI. References

[1] R. T. Conceição, “Avaliação de Desempenho da Operação Conjunta de Múltiplos Conversores Considerando Falhas de Comutação Sucessivas,” Trabalho final de graduação da Univesidade Federal do Rio de Janeiro, Fevereiro/February 2018.

[2] B. Kasztenny, A. Guzmán, N. Fischer, M. V. Mynam, and D. Taylor, “Practical Setting Considerations for Protective Relays That Use Incremental Quantities and Traveling Waves,” proceedings of the 43rd Annual Western Protective Relay Conference, October 2016. Available: selinc.com.

[3] *SEL-T400L Ultra-High-Speed Transmission Line Relay Traveling-Wave Fault Locator High-Resolution Event Recorder Instruction Manual*. Available: selinc.com.

[4] A. Guzmán, G. Smelich, Z. Sheffield, and D. Taylor, “Testing Traveling-Wave Line Protection and Fault Locators,” proceedings of the 14th International Conference on Developments in Power System Protection, Belfast, UK, March 2018. Available: selinc.com

[5] T. R. Honorato, J. P. G. Ribeiro, E. A. Custódio, K. M. Silva, and F. V. Lopes, “Automated Testing Application for a Novel Playback Functionality on a Real Time-Domain Relay,” proceedings of the 15th International Conference on Developments in Power System Protection, Liverpool, UK, March 2020.

VII. Biographies

Denise Borges de Oliveira is from Rio de Janeiro. She graduated in electrical engineering from Universidade do Estado do Rio de Janeiro in 1981 and completed a specialization in power systems protection at the same university in 2003. She worked at Eletrobras Furnas from 1981 to 2013 in analysis and protection studies. In 2014, she joined Operador Nacional do Sistema Elétrico, working on disturbance analysis and protection settings in the protection and control department. She participates in Grupo de Estudos de Proteção (GE03) of Comissão Mista de Operação ANDE/ITAIPU/ ELETROBRAS (CMO). She is an active member of the Comitê de Proteção e Automação (CE B5) at Cigré Brazil.

Tatiana Maria Tavares de Souza Alves received a degree in electrical engineering from Centro Federal de Educação Tecnológica in 2003. In 2005, she completed a specialization in power systems protection at the Escola Politécnica da Universidade Federal do Rio de Janeiro (Poli/UFRJ). She received a Master's degree in Electrical Engineering from COPPE/UFRJ in 2011. She joined Operador Nacional do Sistema Elétrico in 2004 where she is a protection and control management engineer, working in protection studies and disturbance analysis. She is an active member of the Comitê de Proteção e Automação (CE B5) at Cigré Brazil.

Alex Castro received a degree in electrical engineering with an emphasis in electronics from Universidade Federal do Rio de Janeiro in 1994. He worked as an electronics engineer at the Electrical Energy Research Center (Cepel) in the areas of model reduction, modal analysis, small-signal stability, and graphical user interface. He currently works in the direct current systems simulator (HVDC) of Operador Nacional do Sistema Elétrico using RTDS (RSCAD) and offline Power Systems Computer Aided Design (PSCAD) simulation tools and operating replica systems.

Antônio Carlos Duarte received a degree in electrical engineering from Operador Nacional do Sistema Elétrico in 1973. He has a postgraduate degree in electrical systems engineering (CESE) from Universidade Federal de Itajubá (formerly known as Escola Federal de Engenharia de Itajubá) in Minas Gerais, a specialization in power systems protection from Universidad Autónoma de Nuevo León in Mexico, and he has been an instructor of the protection specialization course at Universidade Federal do Rio de Janeiro since 2002. From 1973 to 1982, he worked in the engineering department at Eletrobras Furnas. From 1982 to 1998, he worked at Itaipu Binacional as an engineer and manager of the electric and electronics divisions of the department of maintenance engineering and the operational studies and standards division, and from 1999 to 2019 he worked at Operador Nacional do Sistema Elétrico in disturbance analysis.

Felipe Lopes was born in Campina Grande, Paraíba. He received his BS, MS, doctorate, and postdoctorate degrees in electrical engineering from Universidade Federal de Campina Grande from 2009 to 2018. He is currently an adjunct professor in the department of electrical engineering at Universidade de Brasília (UnB) and coordinator of the mirror group B5.55 at Cigré Brazil. He has worked on research related to electromagnetic transients, power systems protection, and fault location.

Tiago Honorato was born in Brazil in 1992. He received his degree in electrical engineering from Universidade de Brasília (UnB) in 2016. He is currently pursuing a master's degree at UnB. He has worked on research related to power systems protection and digital relay test automation.

Andrei Coelho received a degree in electrical engineering with an emphasis on electrical power systems from Universidade Federal de Itajubá in 2014. He completed a specialization in power systems automation at Instituto Nacional de Telecomunicações in 2019. He has been working in application engineering and technical support at Schweitzer Engineering Laboratories (SEL) since 2014, focusing on transmission and distribution applications, as well as protection, control, and automation for various industrial sectors. He contributes to the development of technical papers and presentations at industry seminars. He is also a course instructor at SEL University.

Paulo Lima received his BSEE in electrical engineering from Federal University of Itajubá, Brazil, in 2012. In 2013, he joined Schweitzer Engineering Laboratories, Inc. (SEL) as a protection application engineer in Brazil. In 2018, he became an application engineering group coordinator, and he has been the regional technical manager for Brazil since 2020. He has experience in the application, training, integration, and testing of digital protective relays. He also provides technical writing and training associated with SEL products and SEL University.